

# Bond Studies of High-Strength Concrete Joints Confined with Stirrups, Steel Fibers, or Fiber-Reinforced Polymer Sheets

Bilal S. Hamad, M.ASCE<sup>1</sup>; and Elias Y. Abou Haidar<sup>2</sup>

**Abstract:** The paper presents a correlation study of the results of three research programs conducted on hooked bars anchored in high-strength concrete (HSC) beam-column joints at the American University of Beirut (AUB). The specimen simulated the rigid connection of a cantilever beam to a column. In two previous programs, the beam-column joint was confined either externally with carbon fiber-reinforced polymer (CFRP) sheets or internally by steel fibers incorporated in the concrete mix. Although stirrups were included in the beam and column elements of the specimens of the two programs, the column stirrups were not extended in the beam-column joint. It was necessary to conduct a third program where confinement of the joint was provided internally by stirrups crossing the critical hooked bars region. Results of the three programs indicated positive effect of the different confining modes on bond strength of the anchored bars and ductility of the load-deflection history. Comparison of the results of the three programs is presented. DOI: 10.1061/(ASCE)ST.1943-541X.0001347. © 2015 American Society of Civil Engineers.

**Author keywords:** Reinforced concrete; High-strength concrete; Bond (concrete to reinforcement); Beam-column joints; Hooked-bar anchorages; Confinement; Fiber-reinforced polymers; Steel fibers; Transverse reinforcement; Concrete and masonry structures.

## Introduction

### *External Confinement of High-Strength Concrete Beam-Column Joints with Fiber-Reinforced Polymer Sheets*

Several research papers are reported in the literature on strengthening or seismic rehabilitation of normal-strength concrete (NSC) beam-column joints, lacking transverse reinforcement, using fiber-reinforced polymer (FRP) composites (El-Amoury and Ghobarah 2002; Antonopoulos and Triantafyllou 2003; Li and Grace Chua 2009; Lee et al. 2010). The joints were subjected to simulated seismic loads. Results of all studies indicated that wrapping the non-seismically detailed NSC joints with glass FRP or carbon FRP (CFRP) sheets enhanced the strength and energy dissipation of the joint and changed the brittle mode of failure to a more ductile mode.

Hamad and Bou Abs (2009) reported on a research program conducted at the American University of Beirut (AUB) to investigate the effect of CFRP sheets confining externally high-strength concrete (HSC) beam-column joints in improving the bond strength and ductility of the mode of failure of hooked bars anchored in the joints. Twelve full-scale beam-column specimens were tested using the strong floor-reaction wall testing facility. A schematic view of the FRP externally confined specimen is shown in Fig. 1.

<sup>1</sup>Professor, Dept. of Civil and Environmental Engineering, American Univ. of Beirut, P.O. Box 11-0236, Riad El Solh, Beirut 1107 2020, Lebanon (corresponding author). E-mail: bhamad@aub.edu.lb

<sup>2</sup>Structural Engineer, Dept. of Civil and Environmental Engineering, American Univ. of Beirut, P.O. Box 11-0236, Riad El Solh, Beirut 1107 2020, Lebanon.

Note. This manuscript was submitted on September 27, 2014; approved on April 28, 2015; published online on July 6, 2015. Discussion period open until December 6, 2015; separate discussions must be submitted for individual papers. This paper is part of the *Journal of Structural Engineering*, © ASCE, ISSN 0733-9445/04015098(10)/\$25.00.

The tensile reinforcement of the beam consisted of two 16-, 25-, or 32-mm bars anchored outside the reinforcement cage of the base column using hooked-bar anchorages. The nominal concrete strength was 60 MPa. The variables in the experimental program included bar size and whether the beam-column joints were externally confined with CFRP sheets or not. The CFRP system used in the study was SikaWrap Hex-230C and the epoxy adhesive used was Sikadur 330. The properties of the unidirectional CFRP sheets were: tensile strength of 3,450 MPa, tensile modulus of 230,000 MPa, elongation of 1.5%, and density of 1.8 g/cm<sup>3</sup>.

The final mode of failure of all specimens with no CFRP wrapping was spalling of the side cover normal to the plane of the hook due to the crushing of the concrete at the inner radius of the bend due to the very high local compressive stress concentrations. Failure of the CFRP sheets was by peeling of the edge of the vertical sheet off the beam surface and/or by tearing or shearing of the sheets. The authors concluded that external confinement with CFRP sheets improved the ductility of the load-deflection history of the beam-column specimens and improved the ultimate stress reached in the anchored bars by an average of 23% as compared with unconfined specimens.

### *External Confinement of HSC Beam-Column Joints with Steel Fibers*

Seismic response of steel fiber (SF) concrete beam-column joints was investigated by several researchers. Some of the reported research used NSC specimens (Gencoglu and Eren 2002; Abbas et al. 2014), and other research used high-performance HSC specimens (Ganesan et al. 2007; Anbuvelan and Subramanian 2014). The specimens in the reported research were either interior or exterior beam-column joints subjected to cyclic loading. The objective was to verify the significance of using steel fibers as an alternative solution for minimizing the density of transverse reinforcement in the joint. Results of all reported studies, whether NSC or HSC, indicated that the addition of steel fibers in plain concrete increased the

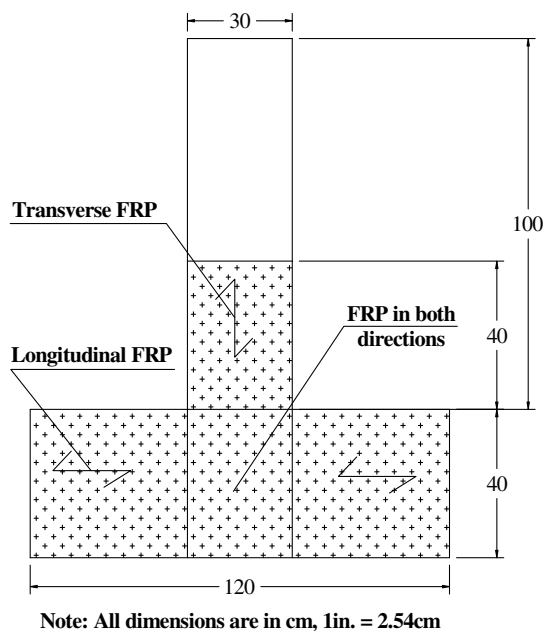


**Fig. 1.** Typical wrapping of the beam-column joint with FRP sheets (reprinted from Hamad and Bou Abs 2009, with permission from the American Concrete Institute)

strength, ductility and stiffness, and energy dissipation capacity of the beam-column joint.

In an earlier phase of the research program reported in this paper, Hamad and Abou Haidar reported on tests of 12 full-scale beam-column joint specimens (Hamad and Abou Haidar 2011) similar in geometry to the ones tested by Hamad and Bou Abs (2009) to assess the viability of steel fibers incorporated in the concrete mix in improving the bond strength of hooked bars anchored in the joints (Hamad and Abu Haidar 2011). The variables were bar size of 16, 25, or 32 mm, and the volume fraction of steel fibers incorporated in the concrete mix,  $V_f$ , was 0, 0.5, 1.0, or 1.5%, where  $V_f$  is the percentage of steel fibers by volume of concrete or the fiber content per cubic meter of concrete. The steel fibers used were Dramix ZP 305 loose hooked steel fibers of type 30 (aspect ratio  $L/d_f = 30/0.55 = 55$ ) provided by Bekaert. The fibers comply with ASTM A820/A820M-06 specifications (ASTM 2006). They have a density of 7,900 kg/m<sup>3</sup>, modulus of elasticity of 207 GPa, and yield stress of 1,100 MPa. The fibers were introduced directly into the mix at the batching plant and were added in 0.5, 1, or 1.5% volume fraction of concrete. The volume fractions correspond to fiber contents of 39.5, 79, and 118.5 kg/m<sup>3</sup> of concrete, respectively. A schematic view of a steel fiber internally confined test specimen is shown in Fig. 2.

Hamad and Abou Haidar (2011) concluded that the confinement effect provided by steel fibers incorporated in the concrete matrix enhanced bond strength and ductility of the mode of failure of the test specimen. The average increases in bond strength relative to the control specimens without fibers were 29, 55, and 61% for the three tested volume fractions of steel fibers 0.5, 1.0, and 1.5%, respectively.

The final mode of failure of all tested specimens was tensile splitting of the concrete cover normal to the plane of the hook accompanied by tensile splitting of the cover in the tension corner zone of the beam-column joint where flexural cracks were initiated. For all three bar sizes tested, the addition of steel fibers in the concrete mix led to increase in the ultimate load of the specimen, increase in the corresponding steel stress, and increase in the ductility

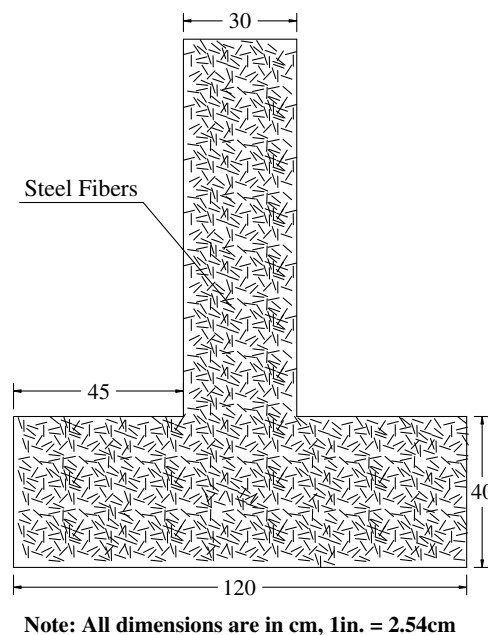


**Fig. 2.** Typical configuration of the beam-column joint with steel fibers

of the load-deflection history. The average increases in the ultimate steel stress reached for the three tested bar sizes were 29% for  $V_f = 0.5\%$ , 55% for  $V_f = 1.0\%$ , and 61% for  $V_f = 1.5\%$ .

## Research Significance

The objective of the research reported in this paper was to evaluate the effect of transverse reinforcement confining HSC beam-column joints on the bond performance of hooked bars anchored in the joint, and to compare the results with the two previous AUB studies in which similar HSC beam-column joints were confined either externally with CFRP sheets or internally with steel fibers incorporated in the concrete mix. Although stirrups were included in the beam and column elements of the specimens of the two earlier programs, the column stirrups were not extended in the beam-column joint. The previous research indicated positive contribution of FRP sheets and steel fibers to the bond strength of the hooked bars anchored in the HSC beam-column joint and to the ductility of the load-deflection history. It was significant to investigate if such improvement would prevail if confinement of the joints is provided internally by transverse reinforcement extending within the joint and crossing the hooked bars rather than FRP sheets or steel fibers. It was also important to perform a correlation analysis of the effects of the three modes of confinement of the HSC beam-column joint within the scope of the studies presented. Results of the study would have an impact on the design and construction of HSC beam-column joints.

## Experimental Program

Nine full-scale HSC beam-column joint specimens with stirrups or ties crossing the hooked bar region were constructed and tested using the floor-reaction wall testing facility. The specimens were identical in geometry to the beam-column specimens of the two previous AUB HSC research programs on beam-column connections that were presented in the introduction. The specimens were designed so that the final mode of failure would be splitting of the side cover normal to the plane of the hook.

The specimen simulated the rigid connection of a cantilever beam to a column. It consisted of a  $30 \times 30$  cm vertical element of height 100 cm, simulating a cantilever beam, anchored in a  $30 \times 40$  cm base 120 cm long, simulating a column. The tensile reinforcement of the beam consisted of two bars anchored outside the reinforcement cage of the base column using hooked-bar anchorages. The hook was detailed according to the standard hook details of the American Concrete Institute (ACI) building code (ACI 2011). The reinforcement on the compression side of the beam consisted of two 10-mm bars in all specimens. The clear concrete cover on the tension and compression sides was 3 cm. In all specimens, the longitudinal reinforcement of the base column consisted of two layers of three 25-mm bars each. Transverse reinforcement was placed in all elements.

To ensure bond splitting failure before the tensile steel bars yield, the embedment depth of the tensile bars of the vertical elements in the base column, as measured from the interface to the outside end of the hook, was chosen in all 12 specimens to be shorter than the basic development length  $l_{dh}$  for a deformed bar terminating in a standard hook, as specified by the ACI building code (ACI 2011)

$$l_{dh} = (0.02\psi_e\lambda f_y / \sqrt{f'_c})d_b \quad (1)$$

where  $\psi_e$  = coating factor;  $\lambda$  = lightweight aggregate concrete factor;  $f_y$  = yield strength of the anchored bars;  $f'_c$  = concrete

**Table 1.** Test Variables

Specimen notation	Tensile beam bar size (mm)	Stirrup spacing
16H	16	—
16H- $3.0d_b$	16	$3.0 \times d_b$
16H- $1.5d_b$	16	$1.5 \times d_b$
25H	25	—
25H- $3.0d_b$	25	$3.0 \times d_b$
25H- $1.5d_b$	25	$1.5 \times d_b$
32H	32	—
32H- $4.0d_b$	32	$4.0 \times d_b$
32H- $2.0d_b$	32	$2.0 \times d_b$

compressive strength; and  $d_b$  = bar diameter. Both factors  $\psi_e$  and  $\lambda$  are 1 in the study. The embedment depths used in the study were 15 cm for the 16- and the 25-mm beam bars and 20 cm for the 32-mm beam bar.

The variables were the beam bar size, 16, 25, or 32 mm, and the amount of transverse reinforcement or stirrups crossing the critical hooked bars region in the base column element of the specimen. For each of the three tested bar sizes, the configurations of the specimens differed by the number and spacing of 10-mm transverse reinforcement or stirrups crossing the critical hooked bar region. The specimens are identified in Table 1. For each size of the beam bars, three specimens identical except for the amount of transverse reinforcement were tested. Schematic views of the 25-mm bar specimens with different stirrups spacing in the beam-column joint are shown in Figs. 3 and 4.

Grade 60 tensile reinforcing bars with the same parallel deformation pattern were used. The bars met ASTM A615/A615M-09 specifications (ASTM 2009). Two coupons of each bar size were tested to confirm the mill test report obtained from the supplier. The average yield stresses were 565 MPa for the 10-mm bars, 700 MPa for the 16-mm bars, 600 MPa for the 25-mm bars, and 510 MPa for the 32-mm bars.

A non-air-entrained concrete mix was designed to give a nominal compressive strength at 28 days of 60 MPa. The mix was provided by a local ready-mix supplier. The water-cement ratio was 0.27. Properties of the mix constituents and the batching weights per cubic meter of concrete are listed in Table 2. The superplasticizer used had 40% solids and a specific gravity of 1.2. The specimens and the corresponding cylinders [ $15.24 \times 30.48$  cm ( $6 \times 12$  in.)] were cured for 7 days.

The specimens were tested using the strong floor-reaction wall testing facility in the materials testing lab. The method of loading simulates the reaction conditions at a beam-column joint. A lateral compressive force was applied through a hydraulic jack mounted on the reaction wall at approximately 15 cm from the tip of the beam while the base was fixed to the strong floor as shown in Fig. 5. The load was applied monotonically in increments of 10 kN until bond failure of the hooked bars occurred. The load and the tip beam

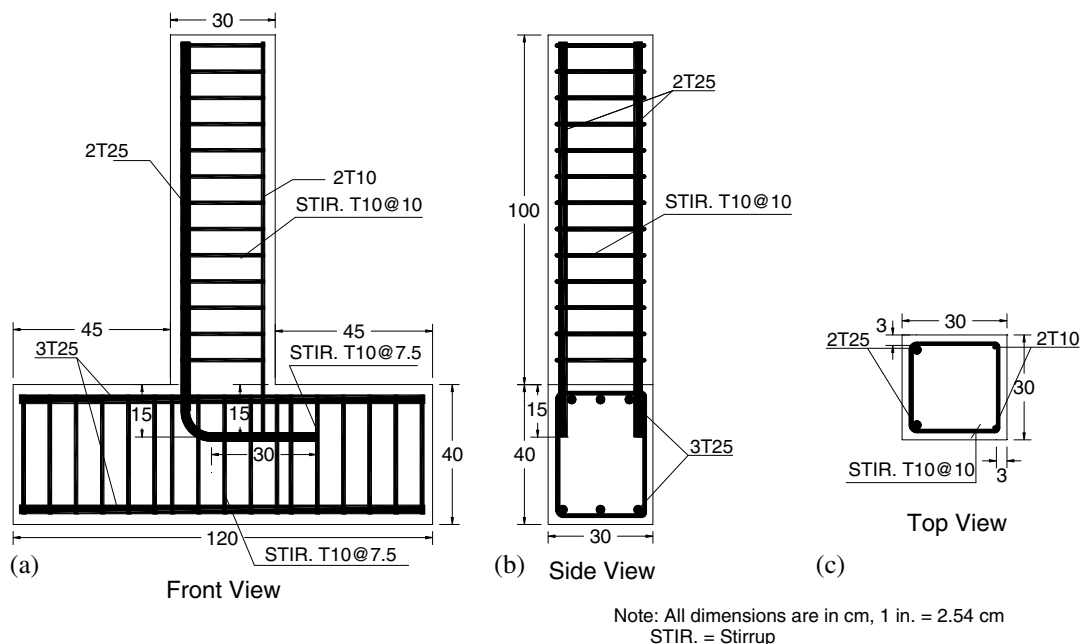


**Fig. 3.** Typical schematic view of the beam-column specimen with 25-mm beam bars and stirrups at  $3.0d_b$ : (a) front view; (b) side view; (c) top view

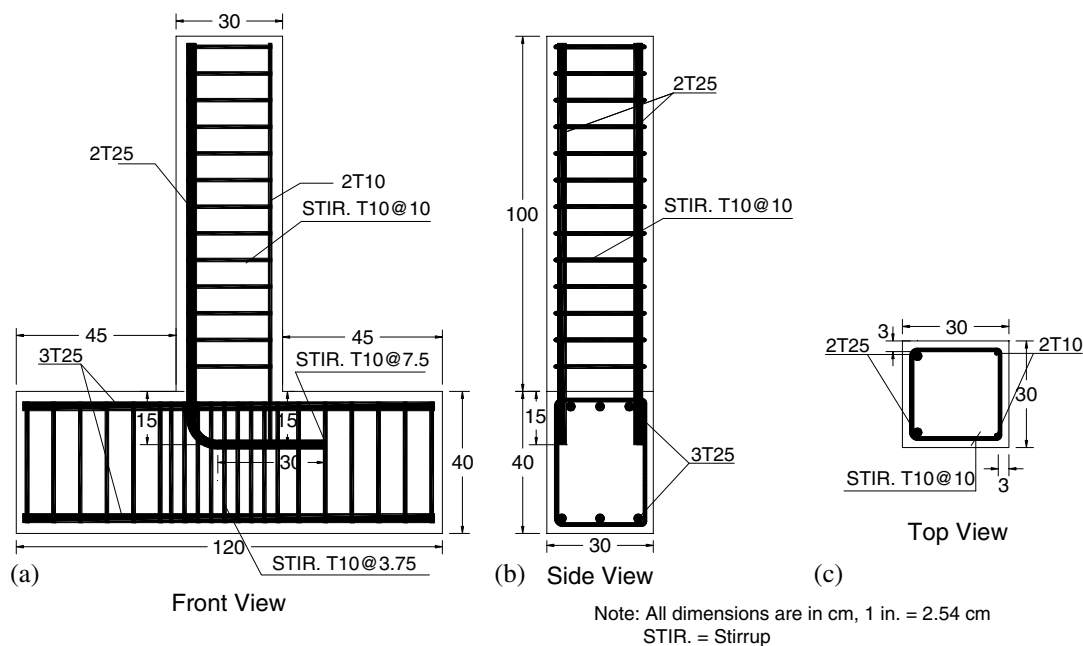


**Fig. 4.** Typical schematic view of the beam-column specimen with 25-mm beam bars and stirrups at  $1.5d_b$ : (a) front view; (b) side view; (c) top view

**Table 2.** Concrete Mix Proportions

Material	Weight per cubic meter of concrete (kg)
Cement, ASTM Type I	450
Fine aggregate (natural sand)	895
Bulk specific gravity = 2.69	
Absorption capacity = 3.2%	
Fineness modulus = 2.4	
Coarse aggregate (crushed limestone)	1,060
Maximum size = 20 mm	
Bulk specific gravity = 2.69	
Absorption capacity = 1.8%	
Silica fume	40
Water	130

deflection at the point of the application of the load were monitored using data acquisition system connected to the testing facility. At each load stage, crack patterns were marked.

### Mode of Failure

In all specimens, the first principal crack was detected at low loading level at the corner of the beam-column interface on the tension side of the beam. Then, the crack tended to intersect the right corner of the beam-column interface at the extreme compression fiber at advanced loading stages. The second principal crack in the base column was diagonal in orientation. It began below the beam-column corner on the tension side and propagated along the anchored hooked bars. Other cracks branched from this diagonal crack in a V pattern toward the top surface of the base element. The cracks also defined the failing concrete zone within the bend of the hooked bars. The final mode of failure was spalling of the side cover normal to the plane of the hook due to the crushing of the concrete at the inner radius of the bend. In parallel to the base column cracks, several beam cracks were observed. The mode of failure was very similar to the mode of the beam-column specimens of the two earlier AUB HSC programs where confinement of the joint was provided by external FRP wrapping or by steel fibers incorporated in the concrete mix (Hamad and Bou Abs 2009; Hamad and Abu Haidar 2011). Typical cracking pattern and mode of failure of the HSC beam-column specimen with 25-mm beam bars and 0.5% steel fibers is presented in Fig. 6.

### Test Results

The effect of transverse reinforcement was evaluated by comparing the performance of the specimens with different amount of transverse reinforcement or stirrups, crossing the critical hooked bars region in the base column element of the specimen, with the companion specimen of the same bar size but without such transverse reinforcement. The comparison was conducted for each of the three bar sizes tested, 16, 25, and 32 mm, and was based on the mode of



**Fig. 5.** View of the test setup (reprinted from Hamad and Abou Haidar 2011, © ASCE)



**Fig. 6.** Typical cracking pattern of the HSC beam-column specimen with 25-mm beam bars and 0.5% steel fibers; cracks shown in dotted lines happened after the specimen reached the maximum load and prior to halting the test (reprinted from Hamad and Abou Haidar 2011, © ASCE)

failure, ultimate load, and general load-deflection behavior. The test data were also compared with the results of the previous research programs, conducted at AUB, on HSC beam-column joints to compare the contributions to the bond strength of the hooked bars of FRP sheets externally wrapping the beam-column joint, steel fibers incorporated in the concrete mix, and stirrups crossing the critical hooked bars region.

To allow direct comparison of all test specimens, the corresponding load-deflection data were normalized to a common concrete strength of 60 MPa. The adjustment was made by multiplying the load at each deflection by  $(60/f'_c)^{1/4}$ , where  $f'_c$  is the concrete strength in megapascals of the specimen under consideration at the day of testing. According to Darwin et al. (1996),  $f'_c^{1/4}$  provides better representation than  $f'_c^{1/2}$  of the effect of concrete strength on bond strength for concretes with compressive strength between 17 and 110 MPa. Test results are presented in Tables 3–5. The measured displacement or deflection is at the point of application of the lateral compressive load.

## Load-Deflection Behavior

### 16-mm-Bar Specimens

The load-deflection curves for the seven tested 16-mm-bar specimens with different confining modes of the beam-column joint are shown in Fig. 7. The curves are almost identical up to a load of approximately 40 kN corresponding to the initiation of the first

**Table 3.** Test Results of the 16-mm Specimens

Specimen	Normalized ultimate load $P_{max}$ (kN) <sup>a</sup>	Displacement at $P_{max}$ (mm)	Ratio of ultimate loads <sup>b</sup>
16H	57.66	7.48	1
16H-3.0 $d_b$	74.02	10.20	1.28
16H-1.5 $d_b$	75.69	15.53	1.31
0.5% SF <sup>c</sup>	79.30	9.24	1.37
1.0% SF <sup>c</sup>	85.98	9.73	1.49
1.5% SF <sup>c</sup>	100.52	10.15	1.74
16H-F <sup>d</sup>	80.24	11.21	1.39

<sup>a</sup>Ultimate loads of the specimens were normalized at a common  $f'_c$  of 60 MPa.

<sup>b</sup>This is the ratio of the ultimate load of a tested specimen of a given bar size and a given amount of stirrups, volume fraction of steel fibers, or FRP sheets to that of the companion specimen with no stirrups, steel fibers, or FRP sheets in the same group.

<sup>c</sup>Specimens with different volume fraction of SFs incorporated in the concrete mix,  $V_f$ .

<sup>d</sup>Specimens with FRP sheets.

**Table 4.** Test Results of the 25-mm Specimens

Specimen	Normalized ultimate load $P_{max}$ (kN) <sup>a</sup>	Displacement at $P_{max}$ (mm)	Ratio of ultimate loads <sup>b</sup>
25H	71.27	10.14	1
25H-3.0 $d_b$	126.53	18.06	1.78
25H-1.5 $d_b$	127.85	22.31	1.79
0.5% SF <sup>c</sup>	101.94	14.07	1.43
1.0% SF <sup>c</sup>	141.22	15.01	1.98
1.5% SF <sup>c</sup>	146.47	15.38	2.05
25H-F <sup>d</sup>	105.61	16.92	1.48

<sup>a</sup>Ultimate loads of the specimens were normalized at a common  $f'_c$  of 60 MPa.

<sup>b</sup>This is the ratio of the ultimate load of a tested specimen of a given bar size and a given amount of stirrups, volume fraction of steel fibers, or FRP sheets to that of the companion specimen with no stirrups, steel fibers, or FRP sheets in the same group.

<sup>c</sup>Specimens with different volume fraction of SFs incorporated in the concrete mix,  $V_f$ .

<sup>d</sup>Specimens with FRP sheets.

**Table 5.** Test Results of the 32-mm Specimens

Specimen	Normalized ultimate load $P_{max}$ (kN) <sup>a</sup>	Displacement at $P_{max}$ (mm)	Ratio of ultimate loads <sup>b</sup>
32H	146.42	24.00	1
32H-4.0 $d_b$	183.75	27.63	1.25
32H-2.0 $d_b$	189.50	26.89	1.29
0.5% SF <sup>c</sup>	166.69	18.39	1.14
1.0% SF <sup>c</sup>	198.94	22.73	1.36
1.5% SF <sup>c</sup>	217.27	22.25	1.48
32H-F <sup>d</sup>	169.60	27.33	1.16

<sup>a</sup>Ultimate loads of the specimens were normalized at a common  $f'_c$  of 60 MPa.

<sup>b</sup>This is the ratio of the ultimate load of a tested specimen of a given bar size and a given amount of stirrups, volume fraction of steel fibers, or FRP sheets to that of the companion specimen with no stirrups, steel fibers, or FRP sheets in the same group.

<sup>c</sup>Specimens with different volume fraction of SFs incorporated in the concrete mix,  $V_f$ .

<sup>d</sup>Specimens with FRP sheets.

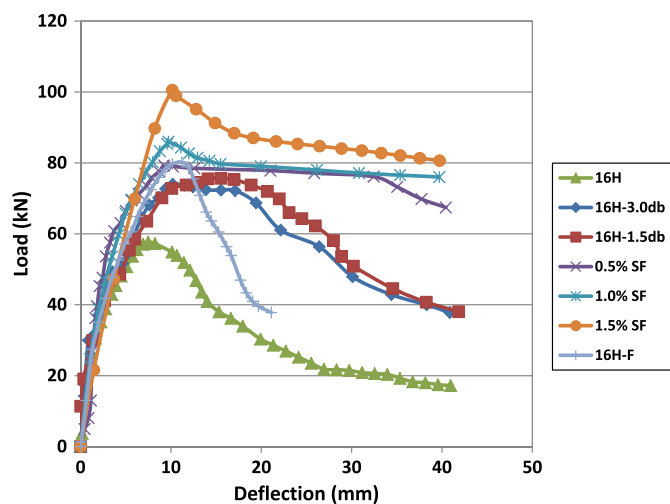


Fig. 7. Load-deflection curves of the 16-mm-bar specimens

principal crack. Above the cracking load, the control specimen 16H with no confinement to the beam-column joint, external or internal, deviates clearly from the other specimens and flattens until a well-defined peak is achieved at a load of 57.66 kN corresponding to a deflection of 7.48 mm.

The other specimens, with transverse reinforcement confining the beam-column joint internally, remained gaining load. The peak for specimen 16H-3.0 $d_b$  was reached at 74.02 kN at a displacement of 10.2 mm, while the peak of 16H-1.5 $d_b$  was reached at 75.68 kN at a displacement of 15.53 mm. The performance of the two specimens with stirrups in the hook region was very similar in ultimate load and load-deflection history with no significant increase noted in the ultimate load as the spacing of stirrups crossing the critical hooked bars region was reduced from 3.0 $d_b$  to 1.5 $d_b$ .

As for the specimens with steel fibers, the ultimate load reached kept increasing as the fiber content increased. The peak for the specimen with 0.5% fiber content was reached at 79.3 kN at a displacement of 9.24 mm, the peak for specimen 1.0% SF was reached at an ultimate load of 85.98 kN with a displacement of 9.73 mm, and the peak for specimen 1.5% SF was reached at an ultimate load of 100.52 kN with a displacement of 10.15 mm. For the FRP specimen 16H-F, the peak was reached at 80.24 kN at a displacement of 11.21 mm.

Taking the area under the load-deflection curve as an indicator of ductility, the different modes of confinement resulted in improvement of the ductility of the load-deflection history of the different beam-column specimens as compared with the control unconfined specimen.

When compared with the control 16-mm-bar specimen 16H, the increases in the ultimate load are 28% for 16H-3.0 $d_b$ , 31% for 16H-1.5 $d_b$ , 38% for 0.5% SF, 49% for 1.0% SF, 74% for 1.5% SF, and 39% for 16H-F (Table 3).

### 25-mm-Bar Specimens

Load-deflection curves for the tested 25-mm-bar specimens with different confining modes of the beam-column joint are shown in Fig. 8. Similar to the 16-mm-bar specimens, the seven curves are almost identical up to the first cracking load of approximately 40 kN. Above the cracking load, the control specimen with no steel fibers, 25H, deviates from the other specimens and reaches a peak at a load of 71.27 kN corresponding to a deflection of 10.14 mm. The other specimens remained gaining load with the curves corresponding to the two specimens with stirrups at 1.5 $d_b$  and 3.0 $d_b$  being similar, and the curves corresponding to the specimens with

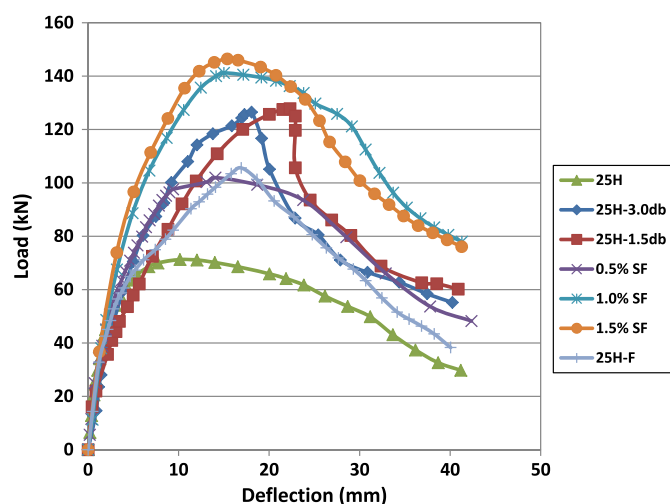


Fig. 8. Load-deflection curves of the 25-mm-bar specimens

steel fibers volume fractions of 1.0 and 1.5% being very similar too. The peak for specimen 25H-3.0 $d_b$  was reached at 126.53 kN at a displacement of 18.06 mm and the peak of 25H-1.5 $d_b$  was reached at 127.85 kN at a displacement of 22.31 mm.

The peak for specimen 0.5% SF was reached at 101.94 kN at a displacement of 14.07 mm, the peak for specimen 1.0% SF was reached at an ultimate load of 141.22 kN with a displacement of 15.01 mm, and the peak for specimen 1.5% SF was reached at an ultimate load of 146.47 kN with a displacement of 15.38 mm. The FRP specimen 25H-F reached a maximum ultimate load of 105.61 kN at a displacement of 16.92 mm.

Similar to the 16-mm-bar specimens, the different modes of confinement resulted in improvement of the ductility of the load-deflection history of the different beam-column specimens as compared with the control unconfined specimen.

The increases in the ultimate load relative to the control specimen with no fibers 25H are 78% for 25H-3.0 $d_b$ , 79% for 25H-1.5 $d_b$ , 43% for 0.5% SF, 98% for 1.0% SF, 106% for 1.5% SF, and 48% for 25H-F (Table 4).

### 32-mm-Bar Specimens

Load-deflection curves for the tested 32-mm-bar specimens are shown in Fig. 9. The seven curves are almost identical up to the

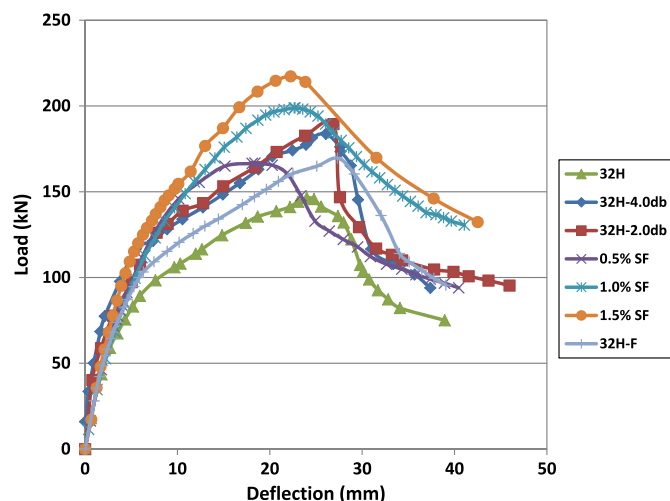


Fig. 9. Load-deflection curves of the 32-mm-bar specimens

first cracking load of approximately 40 kN. Above the cracking load, the control specimen with no steel fibers, 32H, deviates clearly from the other specimens and reaches a peak at a load of 146.42 kN corresponding to a deflection of 24 mm. The other specimens remain gaining load and as with the 16- and 25-mm-bar specimens, no significant increase was noted in the ultimate load as the spacing of stirrups crossing the critical hooked bars region was reduced. The peaks for specimens 32H-4.0 $d_b$  and 32H-2.0 $d_b$  are 183.75 and 189.5 kN, respectively, corresponding to tip beam displacements of 27.63 and 26.89 mm, respectively. The curves corresponding to the two specimens are also similar in this case.

The peaks for the specimens 0.5% SF, 1.0% SF, and 1.5% SF are 166.69, 198.94, and 217.27 kN, respectively. The latter ultimate loads correspond to tip beam displacements of 18.39, 22.73, and 22.25 mm, respectively. The FRP specimen, 32H-F, reached an ultimate load of 169.6 kN at a displacement of 27.33 mm.

Similar to the 16- and 25-mm-bar specimens, the different modes of confinement resulted in improvement of the ductility of the load-deflection history of the different beam-column specimens as compared with the control unconfined specimen.

When compared with the control 32-mm-bar specimen, 32H, the increases in the ultimate load are 25% for 32H-4.0 $d_b$ , 29% for 32H-2.0 $d_b$ , 14% for 0.5% SF, 36% for 1.0% SF, 48% for 1.5% SF, and 16% for 32H-F (Table 5).

### Stress-Strain Modeling and Computation of Steel Stresses

Stress-strain analysis of the beam cross section at the beam-column interface was performed at the level of the normalized ultimate load reached for all specimens.

On the compression side, concrete was assumed to have the following stress-strain relationship as proposed by Scott et al. (1982):

$$f_c = f'_c \left[ \frac{2\varepsilon_c}{0.002} - \left( \frac{\varepsilon_c}{0.002} \right)^2 \right] \quad (2)$$

The stress-strain model represented by Eq. (2) was first suggested by Kent and Park (1971) based on the existing experimental data for concrete confined by rectangular hoops (stirrups) and up to a concrete strain of 0.002. This approach was then adopted by Scott et al. (1982), and the equation was presented in Section 2.1.3 in Chapter 2 of Park and Paulay (1975).

The compressive concrete force was calculated based on the dissection of the stress diagram in the compression zone into ten trapezoidal parts and computing the stress at each point using Eq. (2). The sum of the trapezoidal areas is multiplied by the beam width in order to obtain the compressive force  $C_c$ . On the other hand, the steel compression force is given as follows:

$$C_s = A'_s \cdot f'_s = A'_s \cdot E_s \cdot \varepsilon'_s \quad \text{where } \varepsilon'_s = \left[ \frac{(kd - d'_s)}{kd} \varepsilon_c \right] \quad (3)$$

On the tension side, the main beam reinforcing bars  $T_s$  is defined as by Eq. (4)

$$T_s = A_s \cdot f_s = A_s \cdot E_s \cdot \varepsilon_s \quad \text{where } \varepsilon_s = \left[ \frac{(d - kd)}{kd} \varepsilon_c \right] \quad (4)$$

Two equations are required to solve for the two unknowns ( $kd$  and  $\varepsilon_c$ ). The first equation is the result of equating the sum of the compression forces  $C_c$  and  $C_s$  to the tensile force  $T_s$

$$C_c + A'_s \cdot E_s \cdot \left[ \frac{(kd - d'_s)}{kd} \varepsilon_c \right] = A_s \cdot E_s \cdot \left[ \frac{(d - kd)}{kd} \varepsilon_c \right] \quad (5)$$

The second equation is obtained by equating the external moment  $M_{ext}$ , calculated by multiplying the normalized ultimate load reached by each specimen by the moment arm [85 cm (33.5 in.)], to the internal moment  $M_{int}$ , calculated using stress-strain analysis

$$M_{ext} = M_{int} = C_c \cdot \bar{x} + C_s \cdot (kd - d'_s) + T_s \cdot (d - kd) \quad (6)$$

The values for the strain in the outermost concrete compression fiber  $\varepsilon_c$  and the neutral axis location  $kd$  are attained after running the goal seek option in the Microsoft Excel. The values are listed in Table 5. Using the obtained values of  $\varepsilon_c$ , the value of  $\varepsilon_s$  is computed and the steel stress is computed using Eq. (7)

$$f_s = E_s \cdot \varepsilon_s = E_s \cdot \left[ \frac{(d - kd)}{kd} \varepsilon_c \right] \quad (7)$$

The values of  $f_s$  at ultimate load are listed in Table 6 for all tested specimens. Examples of the stress-strain analysis of the two 25-mm-bar specimens, the control specimen with no confinement 25H and the specimen with stirrups crossing the hooked bar region at a spacing of 1.5 $d_b$  (25H-1.5 $d_b$ ), are shown in Figs. 10 and 11. The strain values shown in the figures were determined using the equations listed in this section.

### Bond Ratios

The steel stress values listed in Table 6 indicate that the internal confinement of the hooked bars, provided by the incorporation of transverse reinforcement in the critical hooked bars region, led to an improvement in the level of the steel stress at the maximum

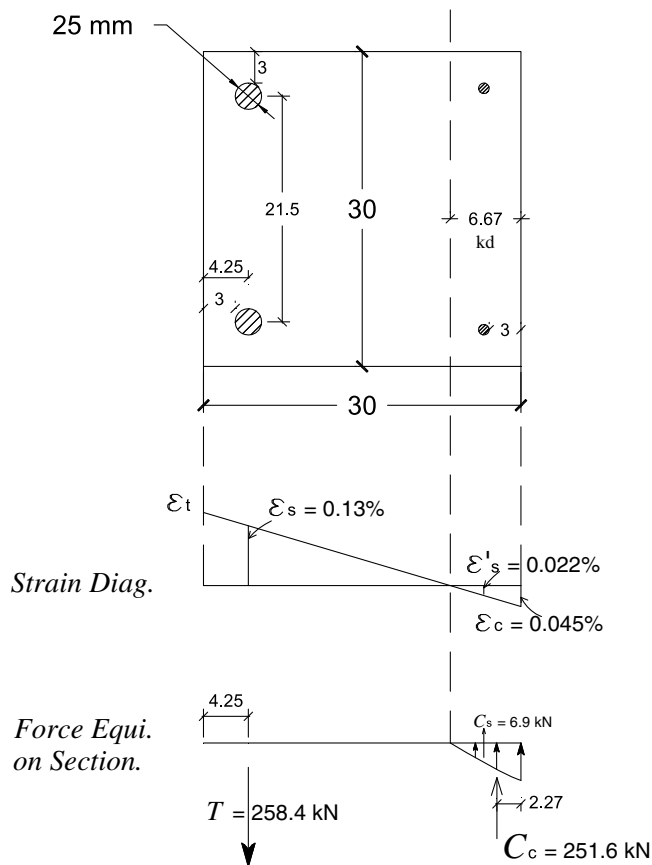
**Table 6.** Strains, Stresses, and Stress Bond Ratios

Specimen notation	Effective depth $d$ (cm)	$kd^a$ (cm)	$\varepsilon_c^a$	$\varepsilon_s$	$f_s$ (MPa)	BR <sup>b</sup>
16H	26.2	4.59	0.00052	0.00244	495.8	—
16H-1.5 $d_b$	26.2	4.65	0.00069	0.00321	651.7	1.31
16H-3.0 $d_b$	26.2	4.58	0.00067	0.00315	639.0	1.29
16H-0.5% SF	26.2	4.59	0.00072	0.00322	654.8	1.32
16H-1.0% SF	26.2	4.77	0.00077	0.00336	682.3	1.38
16H-1.5% SF	26.2	4.90	0.00087	0.00381	700.0	1.41
16H-F	26.2	5.69	0.00086	0.00308	647.8	1.31
25H-0	25.8	6.67	0.00045	0.00130	263.3	—
25H-1.5 $d_b$	25.8	6.88	0.00085	0.00234	474.5	1.80
25H-3.0 $d_b$	25.8	6.88	0.00084	0.00231	469.6	1.78
25H-0.5% SF	25.8	6.84	0.00066	0.00183	371.1	1.41
25H-1.0% SF	25.8	7.05	0.00094	0.00250	507.5	1.93
25H-1.5% SF	25.8	7.13	0.00098	0.00255	518.1	1.97
25H-F	25.8	8.03	0.00083	0.00183	384.2	1.46
32H-0	25.4	8.36	0.00083	0.00170	344.3	—
32H-2.0 $d_b$	25.4	8.55	0.00112	0.00220	447.8	1.30
32H-4.0 $d_b$	25.4	8.52	0.00108	0.00214	434.0	1.26
32H-0.5% SF	25.4	8.48	0.00096	0.00191	388.7	1.13
32H-1.0% SF	25.4	8.67	0.00118	0.00227	461.1	1.34
32H-1.5% SF	25.4	8.80	0.00131	0.00246	499.8	1.45
32H-F	25.4	9.62	0.00115	0.00190	397.7	1.16

Note: All listed values in Table 5 correspond to the maximum or peak loads of the specimens normalized at the common  $f'_c$  of 60 MPa as listed in Tables 3–5.

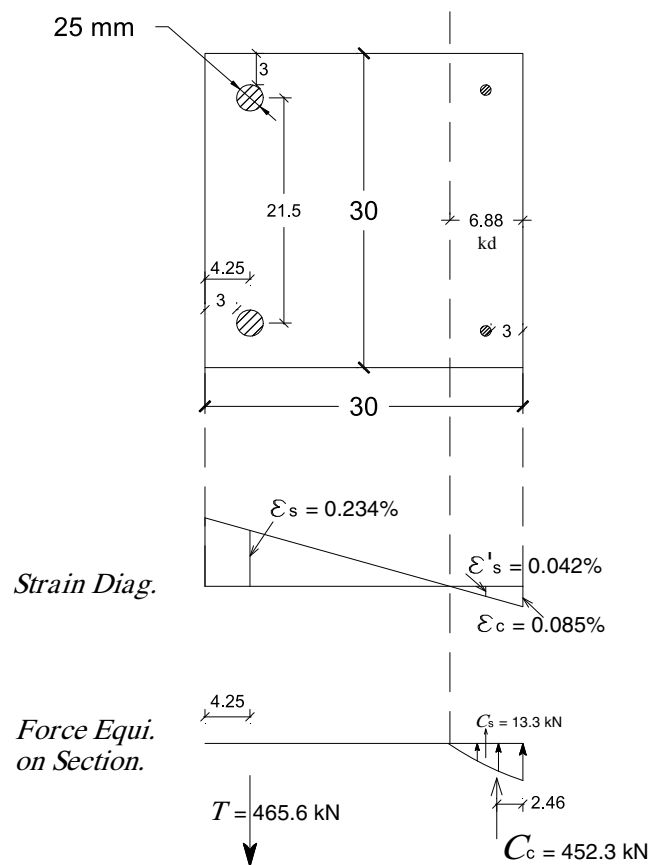
<sup>a</sup>Values of  $kd$  and  $\varepsilon_c$  are obtained by solving Eqs. (5) and (6).

<sup>b</sup>This is the ratio of the steel stress at maximum load of a tested specimen of a given bar size and a given parameter to that of the control specimen in the same group.



NOTE: All measurements are in cm

**Fig. 10.** Stress-strain analysis at ultimate load of the control 25-mm-bar specimen with no confinement (25H) (reprinted from Hamad and Abou Haidar 2011, © ASCE)



NOTE: All measurements are in cm

**Fig. 11.** Stress-strain analysis at ultimate load of the 25-mm-bar specimen with stirrups in the beam-column joint spaced at  $1.5d_b$  (25H- $1.5d_b$ )

load reached. In the two previous AUB research programs (Hamad and Bou Abs 2009; Hamad and Abou Haidar 2011), it was also proven that external confinement of the beam-column joint with FRP sheets and the internal confinement with steel fibers added in the concrete mix both resulted in increase in the steel stress reached by the hooked bars at maximum. The steel stresses of all specimens with different methods of confinement are presented in Table 6.

The bond ratio (BR), whose values are listed in Table 6 for the three tested bar sizes, represents the ratio of the steel stresses at maximum load of a tested specimen confined with one of the three modes of confinement provided to the critical hooked bars region to the steel stress of the control unconfined specimen in the same bar group. The listed bond ratios are illustrated in Figs. 12–14. The plotted histograms or bar graphs clearly indicate that for the three tested bar sizes (16, 25, or 32 mm), all bond ratios are above 1.0 indicating that the different modes of confinement improved the bond strength of the hooked bars with the 1.5% steel fibers specimen performing the best in each category of bar sizes.

Reducing the spacing of transverse reinforcement crossing the critical hooked bars region did not result in significant increase in the steel stress at maximum load reached. However, increasing the volume fraction of steel fibers from 0.5 to 1.5% resulted in consistent increase in steel stress at maximum load.

Whereas the 16-mm specimens with different transverse reinforcement spacings performed similar to the 0.5% steel fibers specimen, the 25- and 32-mm specimens with different transverse reinforcement spacings performed better than the 0.5% steel fibers

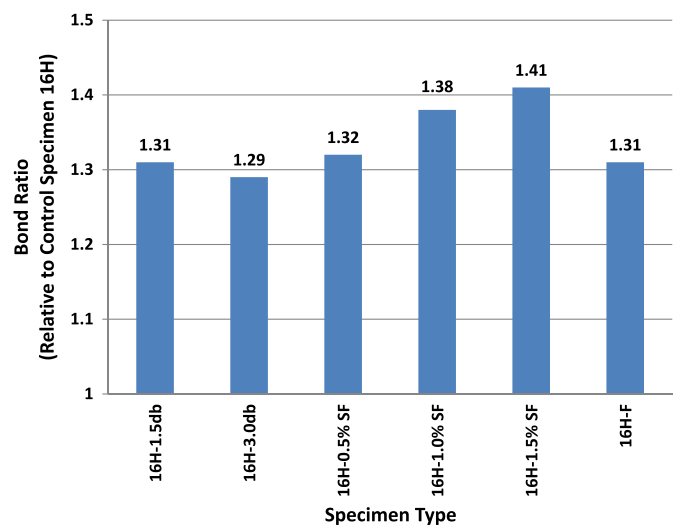


**Fig. 12.** Bond ratios of the 16-mm-bar specimens with different confinement modes to the beam-column joint relative to the control specimen with no confinement

specimen and closer although a little inferior to the 1.0% steel fibers specimen. On the other hand, whereas the 16-mm-bar specimen with FRP wrapping performed similar to the specimens with transverse reinforcement crossing the hooked bar region, the 25- and

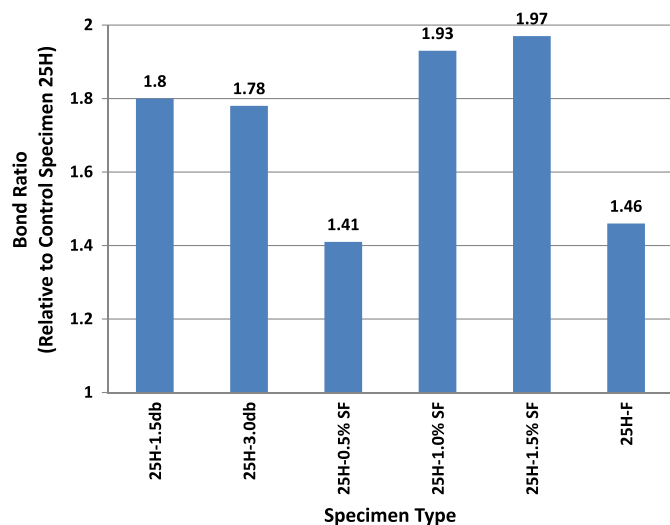


**Fig. 13.** Bond ratios of the 25-mm-bar specimens with different confinement modes to the beam-column joint relative to the control specimen with no confinement

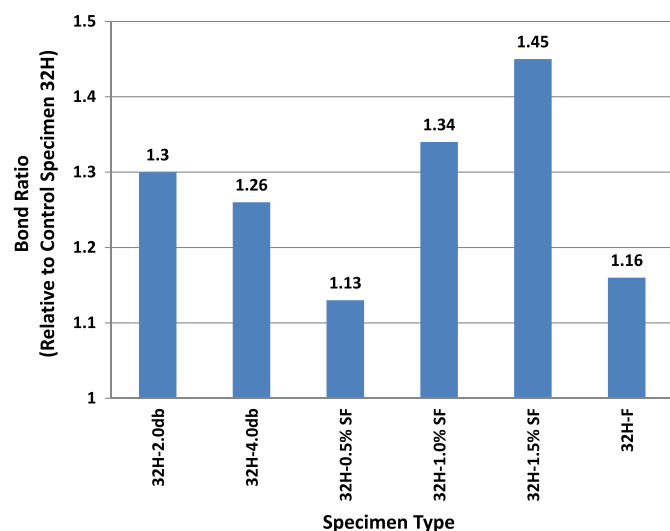


**Fig. 14.** Bond ratios of the 32-mm-bar specimens with different confinement modes to the beam-column joint relative to the control specimen with no confinement

32-mm-bar specimens with FRP wrapping performed inferior to the transverse reinforcement specimens but similar to the 0.5% steel fibers specimens.

## Summary and Conclusions

Based on the test results of the study presented in this paper, the following conclusions could be made:

- The crack patterns of all specimens were similar. The final mode of failure of all specimens was spalling of the side cover normal to the plane of the hook due to the crushing of the concrete at the inner radius of the bend.
- The results indicate the significant and positive effect of transverse reinforcement confinement in improving the bond performance of HSC beam-column connections. For all three bar sizes tested, the addition of stirrups in the beam-column joint crossing

the critical hooked bars region led to increase in the ultimate load of the specimen and the ductility of the load-deflection history. However, whereas increasing the volume fraction of steel fibers from 0.5 to 1.5% resulted in consistent increase in steel stress at maximum load, no significant improvement was reached when the spacing of the stirrups crossing the critical hooked bars region was reduced.

- The three modes of confinement of the HSC beam-column joints, namely CFRP sheets externally wrapping the joint or steel fibers incorporated in the concrete mix or transverse reinforcement crossing the hooked bars region, improved the bond strength characteristics of the tested specimens. The specimen with 1.5% steel fibers performed the best in each category of bar sizes.
- Within the scope of the three conducted HSC research programs, the internal confinement of the 25- and 32-mm-bars beam-column joints with stirrups or steel fibers with volume fractions of 1.0 and 1.5% would better improve the ultimate strength of the joint than external confinement with FRP sheets.
- For the three bar sizes tested, the bond strength of specimens confined internally with transverse reinforcement crossing the critical hooked bar region is similar but a little inferior to specimens with 1.0% steel fibers volume fraction.

## Acknowledgments

The authors gratefully acknowledge Hussein Mallat, Professor Hamad's graduate student at AUB, who was working on his M.S. degree when he had to leave for the United States for cancer treatment and was out of reach during the preparation of the paper. Also, the authors acknowledge the University Research Board at the American University of Beirut for supporting this program.

## Notation

The following symbols are used in this paper:

- $A_c$  = area of compressive strength underneath the stress diagram; the compression zone is dissected into several trapezoidal parts;
- $A_s$  = area of the reinforcing bars on the tension side;
- $A'_s$  = area of steel on the compression side, 2T10 in all cases or 1.57 cm<sup>2</sup>;
- $A_{sf}$  = area of effective steel fibers in the tensile region of the stress-strain diagram;
- BR = bond ratio of steel stresses corresponding to ultimate loads of specimens with different types of confinement relative to control specimen in the same bar group;
- $b_w$  = width of the web of the rectangular beam section = 30 cm (11.8 in.) for all specimens;
- $C_c$  = resultant compressive concrete force;
- $C_s$  = force in steel on the compression side =  $A'_s \cdot f'_s$ ;
- $d$  = effective depth measured from the top fibers in compression to the center of gravity of the tension rebars;
- $d_b$  = bar diameter;
- $d'_s$  = distance from extreme compression fiber to the centroidal axis of compression steel = 3.5 cm (1.38 in.) for all specimens;
- $E_s$  = modulus of elasticity of reinforcing steel bars and steel fibers = 207 GPa (30,000 ksi);
- $f_c$  = stress in concrete at any section;
- $f'_c$  = 28-day compressive strength of concrete under proper conditions of curing and compaction that is normalized to a representative value of 28 MPa (4,061 psi);

$f_s$  = stress in steel at on the tension side at service load level;  
 $f'_s$  = stress in steel on the compression side at service load level;  
 $f_y$  = yield stress of steel;  
 $h$  = section's depth = 30 cm (11.8 in.) for all sections;  
 $kd$  = distance from the exterior compression fiber to the neutral axis of a cracked section;  
 $l_{dh}$  = provisional development length for the main hooked steel bar;  
 $M_{ext}$  = moment at beam-column interface = 85 cm (33.5 in.)  $\times$  normalized ultimate load;  
 $M_{int}$  = moment at beam-column interface calculated using stress-strain analysis;  
 $T_s$  = tension force in main steel;  
 $V_f$  = volume fraction of steel fibers;  
 $\bar{x}$  = distance from the location of the resultant concrete compressive force  $C_c$  to the neutral axis;  
 $\epsilon_c$  = strain in concrete at the extreme compression fiber;  
 $\epsilon_{cu}$  = strain in concrete that causes concrete to crush = 0.002;  
 $\epsilon_s$  = strain in tension steel at its centroidal axis;  
 $\epsilon'_s$  = strain in compression steel at its centroidal axis; and  
 $\epsilon_t$  = strain at the extreme tension fiber.

## References

- Abbas, A., Syed Mohsin, S., and Cotsovos, D. (2014). "Seismic response of steel fibre reinforced concrete beam-column joints." *Eng. Struct. J.*, 59, 261–283.
- ACI (American Concrete Institute). (2011). "Building code requirements for reinforced concrete and commentary." *ACI-318-11/ACI-318R-11*, Farmington Hills, MI.
- Anbuvelan, K., and Subramanian, K. (2014). "Behavior of high performance steel fiber reinforced concrete in exterior beam-column joint—A general review." *Aust. J. Basic Appl. Sci.*, 8(7), 215–219.
- Antonopoulos, C. P., and Triantafillou, T. C. (2003). "Experimental investigation of FRP-strengthened RC beam-column joints." *J. Compos. Constr.*, 10.1061/(ASCE)1090-0268(2003)7:1(39), 39–49.
- ASTM. (2006). "Standard specification for steel fibers for fiber-reinforced concrete." *A820/A820M-06*, West Conshohocken, PA.
- ASTM. (2009). "Standard specification for deformed and plain carbon-steel bars for concrete reinforcement." *A615/A615M-09*, West Conshohocken, PA.
- Darwin, D., Zuo, J., Tholen, M. L., and Idun, E. K. (1996). "Development length criteria for conventional and high relative area reinforcing bars." *ACI Struct. J.*, 93(3), 347–359.
- El-Amoury, T., and Ghobarah, A. (2002). "Seismic rehabilitation of beam-column joint using GFRP sheets." *Elsevier Eng. Struct. J.*, 24(11), 1397–1407.
- Ganesan, N., Indira, P. V., and Abraham, R. (2007). "Steel fibre reinforced high performance concrete beam-column joints subjected to cyclic loading." *ASET J. Earthquake Technol.*, 44(3–4), 445–456.
- Gencoglu, M., and Eren, I. (2002). "An experimental study on the effect of steel fiber reinforced concrete on the behavior of the exterior beam-column joints subjected to reversal cyclic loading." *Turk. J. Eng. Environ. Sci.*, 26, 493–502.
- Hamad, B., and Abou Haidar, E. (2011). "Effect of steel fibers on bond strength of hooked bars in high strength concrete." *J. Mater. Civ. Eng.*, 10.1061/(ASCE)MT.1943-5533.0000230, 673–681.
- Hamad, B., and Bou Abs, C. (2009). "Effect of FRP confinement on bond strength of hooked bars in high strength concrete." *ACI Struct. J.*, 106(6), 831–839.
- Kent, D. C., and Park, R. (1971). "Flexural members with confined concrete." *J. Struct. Div.*, 97(ST7), 1969–1990.
- Lee, W. T., Chiou, Y. J., and Shih, M. H. (2010). "Reinforced concrete beam-column joint strengthened with carbon fiber reinforced polymer." *Compos. Struct. J.*, 92(1), 48–60.
- Li, B., and Grace Chua, H. Y. (2009). "Seismic performance of strengthened reinforced concrete beam-column joints using FRP composites." *J. Struct. Eng.*, 10.1061/(ASCE)0733-9445(2009)135:10(1177), 1177–1190.
- Park, R., and Paulay, T. (1975). *Reinforced concrete structures*, Wiley, New York.
- Scott, B. D., Park, R., and Priestly, M. N. (1982). "Stress-strain behavior of concrete confined by overlapping hoops at low and high strain rates." *ACI Struct. J.*, 79(1), 13–27.